ELSEVIER

PII: S0032-3861(97)00166-3

Polymer Vol. 38 No. 25, pp. 6135–6143, 1997

0032-3861/97/$17.00+0.00

Poly(3-hydroxybutyrate)/poly(methyleneoxide) blends: thermal, crystallization and mechanical behaviour

Maurizio Avella, Ezio Martuscelli*, Giuseppe Orsello and Maria Raimo
Istituto di Ricerca e Tecnologia delle Materie Plastiche Via Toiano 6, 80072 Arco Felice, Napoli, Italy

and Beniamino Pascucci
Consorzio sulle Applicazioni dei Materiali Plastici e per i problemi di Difesa dalla Corrosione, Via Pietro Castellino, 111 80100, Napoli, Italy
(Revised 3 February 1997)

Blends of poly(3-hydroxybutyrate) (PHB)/poly(methylene oxide) (POM) were prepared by melt mixing and subsequent compression moulding. Crystallization, thermal behaviour, morphology and mechanical properties of the blends were studied by using differential scanning calorimetry, optical and scanning electron microscopy, and dynamic-mechanical analysis. The immiscibility of the two polymers in the liquid state was demonstrated. Moreover, two distinct spherulitic phases were evidenced in the solid state and changes of the texture structure with the composition were also observed. Finally, tensile and impact tests were carried out in order to establish the mechanical behaviour of the blends. © 1997 Elsevier Science Ltd.

(Keywords: blends; properties; crystallization)

INTRODUCTION

Poly(3-hydroxybutyrate) (PHB) and poly(methylene oxide) (POM) are two semicrystalline polymers having almost the same melting point (≅ 175°C).

In previous work[1,2,3], the distinctive crystallization behaviour and the miscibility of poly(ethylene oxide) (PEO) and PHB have been deeply investigated. It has been demonstrated that PHB and PEO are miscible in the melt.

Moreover, the high purity of the bacterial PHB[4] allowed study of the nucleation process of PHB/PEO blends crystallized from melt under different crystallization conditions[3].

Unlike PHB and POM, PHB and PEO have very different melting points (≈ 175 and ≈ 60°C respectively), so PHB can be crystallized at temperatures higher than the melting point of PEO, where PEO is still in the liquid phase. This circumstance made possible study of the influence of PHB crystallization on the subsequent PEO crystallization at lower temperatures. It has been shown that in the presence of PHB, PEO crystallization takes place in two steps at different levels of supercooling. This phenomenon, so-called 'fractionated crystallization', was attributed to the occurrence of two different types of nucleation of the PEO during the cooling from melt, a heterogeneous nucleation at lower supercooling and a homogeneous one at higher supercooling. This latter is possible for PEO only in the presence of PHB, as a consequence of the migration of impurities, acting as nucleating centres, from PEO to PHB.

* To whom correspondence should be addressed

In the case of PHB/POM blends, by cooling the melt it is possible to crystallize the POM, leaving the PHB phase in the liquid state. This latter has to be cooled to much lower temperatures before it crystallizes. Thus PHB/POM blends offer the opportunity to study the influence of the POM crystallization on the subsequent crystallization process of the PHB.

The crystallization process is a very important tool to determine the morphology and the mechanical properties of a blend. This work was undertaken aiming at two main objectives: firstly to increase the data concerning the miscibility between PHB and polyethers; secondly, to study the crystallization, and thermal and mechanical behaviour of PHB/POM blends.

EXPERIMENTAL

Materials

PHB, having a molecular mass of 400 000, was supplied by Zeneca Bioproducts, England. POM homopolymer (M_w = 41 000) was provided by Polysciences. In order to indicate the different compositions of the blends, the following codes were used: PHB 20; PHB 40; PHB 60; PHB 80, where the numbers refer to the PHB weight percentage in the blends. PHB and POM codes were used to indicate the neat components of the blend.

Sample preparation

The blends were prepared by using a Brabender Rheocord Apparatus. Appropriate amounts of the two polymers were mixed at 180°C for 5 min with a roll speed

of 32 rpm. Afterwards, the blended material was cooled in liquid nitrogen, and milled using a grinding mill. The resulting material was dried under vacuum in a stove at 80°C until it reached a constant weight. Finally, it was hot-compression-moulded at a temperature of 180°C and a pressure of 15 Gpa for 3 min, and then solidified by water-cooling.

Sheets of thickness 1 mm were cut to obtain dumb-bell specimens for tensile tests. From thinner films (thickness 0.2 mm), strips (60 mm in length × 1 mm in width) were obtained to perform dynamic-mechanical tests.

Impact tests were carried out on samples 60 mm × 6.0 mm in dimension, cut from 3.5 mm thick sheets. The specimens were notched at the middle of their length as follows: first a blunt notch was made with a V-shaped machine tool and then a sharp notch 0.2 mm deep was produced by a razor blade fixed on a micrometric apparatus.

Techniques

Thermal analysis was performed using a Mettler TA-3000 differential scanning calorimeter (d.s.c.) equipped with a control and programming unit and a calorimetric cell operating under a nitrogen atmosphere. Two different procedures were developed:

(A) *Non-isothermal crystallization.* The samples were submitted to the following thermal treatment: first, heating from 30 to 200°C (I RUN), then cooling from 200 to −50°C (CRYSTALLIZATION RUN) and finally re-heating from −50 to 200°C (III RUN). A scan rate of 10°C min^{-1} was used.

(B) *Isothermal crystallization.* The samples were melt up to 200°C and kept at this temperature for two min; then the temperature was quickly (scan rate 50°C min^{-1}) cut down to 153°C. The samples were kept under this condition for 60 min, to ensure the complete crystallization of POM. Afterwards, they were cooled with a scan rate of 50°C min^{-1} at 120°C, to allow the crystallization of the PHB phase.

The crystallized specimens were submitted to scanning electron microscopic (SEM) analysis. A Leitz polarizing optical microscope equipped with a Mettler hot stage (precision ± 0.2°C) was used to follow the course of the crystallization.

The specimens for microscopic observations were prepared by putting on a slide a small amount of blend, heating to melt the specimens, and then overlaying with a cover glass. The two components were first melted, then separately crystallized at temperatures close to 150 and 90°C respectively.

In order to destroy any traces of previous crystallinity, the crystallization from melt was performed after a permanence at 200°C for 2 min.

Micrographs were taken at appropriate times during the isothermal crystallization to measure the radius of the spherulites, and thus report this latter as a function of time. The slope of the resulting straight line is the radial growth rate G of the spherulites.

The melting temperature was determined by heating the samples at 3°C min^{-1} and selecting the temperature at which the birefringence disappears.

SEM was carried out by using a Philips 501 SEM after metallization under vacuum of the samples by means of a Polaron sputtering apparatus with an Au–Pd alloy. Dynamic mechanical measurements were carried out by using a viscoelastomer from 'Toyo Instruments Co. Ltd', the Rheovibron I. The work frequency was 110 Hz. The temperature range was −100 to 100°C.

An Instron machine was used to perform room temperature tensile tests according to ASTM standard methods. The cross head speed adopted was 1 mm min^{-1}.

The impact tests were carried out at room temperature and impact speed of 1 m s^{-1} by using an instrumented pendulum (Ceast Autographic Pendulum MK2). The tests were conducted according to ASTM-D256 standard methods. All the mechanical parameters reported in this work were derived averaging six experimental values for each composition.

MORPHOLOGY OF PHB/POM BLENDS

Observations carried out by optical and electron microscopy on specimens crystallized from melt showed that the morphology of PHB/POM blends strongly depends on the composition.

The observed samples were submitted to the crystallization procedure described in the experimental part, consisting of the two following steps:

1. isothermal crystallization of the POM phase from a heterogeneous melt (crystallization temperatures ≥ 150°C);
2. isothermal crystallization of the PHB from the survived liquid phase in the presence of previously crystallized POM (crystallization temperatures ≤ 120°C).

It is known that kinetic factors make a polymer able to crystallize only at temperatures well below the melting point[5]. In other words, a certain minimum 'supercooling' is needed to crystallize a polymer, and the crystallization from melt does not take place until the requested supercooling is achieved.

In the case of PHB/POM blends, the isothermal two-step crystallization described above is possible because POM and PHB need very different supercoolings to crystallize.

Thus, low supercoolings ($T \geq 150$°C) allow only the POM to crystallize, while the crystallization of the PHB is still kinetically hindered.

Isothermal PHB crystallization may be obtained by cooling to temperatures below 120°C.

The selected crystallization temperature of PHB for optical observations was 90°C, a value corresponding to a rather fast, but still isothermal crystallization.

Morphology arising from the first step of the crystallization procedure

The observation by optical microscopy of films of the blends in the molten state showed two separated phases for almost all of the compositions prepared.

As an example, the phase separation occurring in PHB 40 melt is shown in *Figure 1a*. Droplets of PHB, whose size ranges from tens to hundreds of micrometers, are dispersed in a liquid matrix of POM. *Figure 1b* illustrates the POM spherulites growing at 151°C from the molten phase. The spherulites of POM may grow undisturbed, until they impinge one another or upon the edge of the liquid domains of PHB. In this case, further growth of the spherulites of POM is not allowed in the direction of the impingement, and the circular shape of spherulites is compromised.

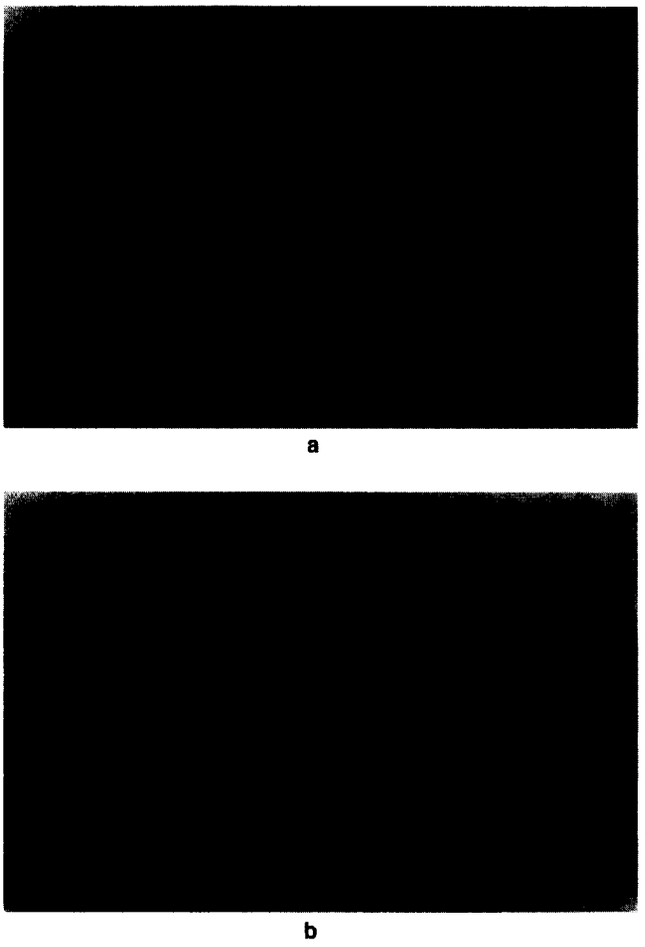

Figure 1 Optical micrographs of PHB 40: (a) incipient crystallization from the melt; (b) growth of POM spherulites at 151°C. Magnification 125×

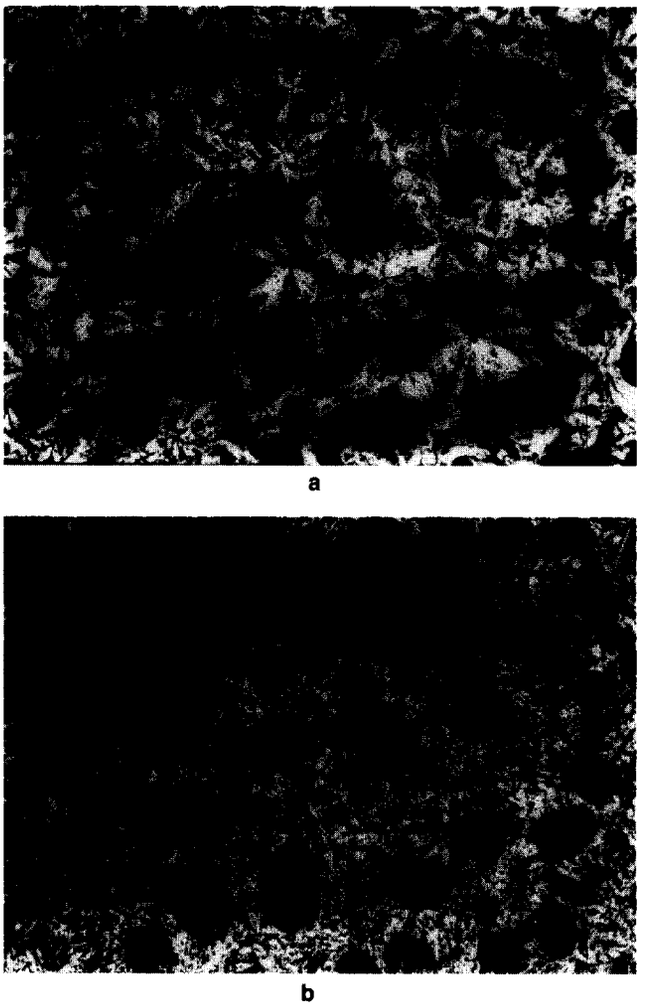

Figure 2 Optical micrographs taken at crossed polaroid: (a) sample of PHB 40 partially crystallized at 151°C; (b) the same region after crystallization of PHB at 90°C. Magnification 100×

An optical crossed polar micrograph, showing POM spherulites grown at 151°C from the heterogeneous melt of PHB 40 blend once the impingement is complete, is reported in *Figure 2a*. The film sample appears as a continuous crystalline phase of POM inglobing dispersed liquid droplets of PHB.

Morphological analysis of blends richer in PHB than PHB 40 has shown a fine dispersion of separated POM droplets (up to 5 μm in diameter) in a PHB matrix. Thus a phase inversion occurs. As shown by *Figure 3a* in the case of film of PHB 60 blend, the first crystallization step at 151°C produces POM spherulites dispersed in a continuous liquid medium of PHB.

Concerning PHB 20 blend, no optical evidence of phase separation in the melt has been observed. Moreover, the POM crystallization during the permanence at the higher temperatures proceeds until the impingement of the spherulites and no liquid domains are visible after its complete crystallization. The further diminution of the temperature does not cause morphological change in the crystalline phase, at least on the level of the observation scale.

Samples morphology after the PHB crystallization according to the second stage of the crystallization procedure

Figure 2b shows the appearance of a sample of PHB 40 blend after the isothermal crystallization of both components. In this case PHB is the minor component of the blend and crystallizes in domains immersed in a matrix of POM spherulites. *Figure 2b* refers to *Figure 2a* where the domains of PHB were still liquid.

The feature of a sample of PHB 60 after the POM crystallization is reported in *Figure 3a*, while in *Figure 3b* is shown the same area after the subsequent PHB crystallization.

MICROSCOPIC STUDIES

Owing to the particular blend morphology, it was possible to lead kinetical studies on the growth rate, G, of POM spherulites only for PHB 20 and PHB 40, where POM constitutes the matrix of the blends. As a matter of fact, a fine dispersion of POM droplets in the PHB matrix is observed in the melt for compositions richer in PHB. The subsequent POM crystallization from this melt structure gives rise to a microspherulitic texture, making it impossible to follow the radial growth of spherulites.

Moreover, it was not possible to calculate the growth rate of PHB spherulites in the blends, because they inglobe the pre-existing crystallized POM phase, hiding their growing front and so making their radius unmeasurable.

The growth rate, G, of POM spherulites for neat POM, PHB 20 and PHB 40, vs the crystallization temperature T_c is illustrated in *Figure 4*.

a

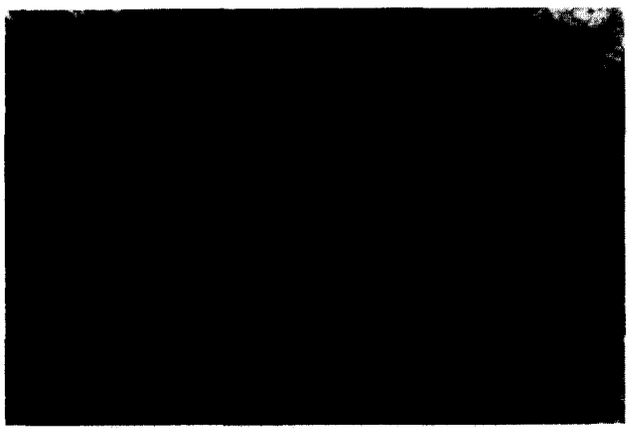

b

Figure 3 Optical micrographs of PHB 60 isothermally crystallized first at 151°C (a), and then at 90°C (b). Magnification 280×

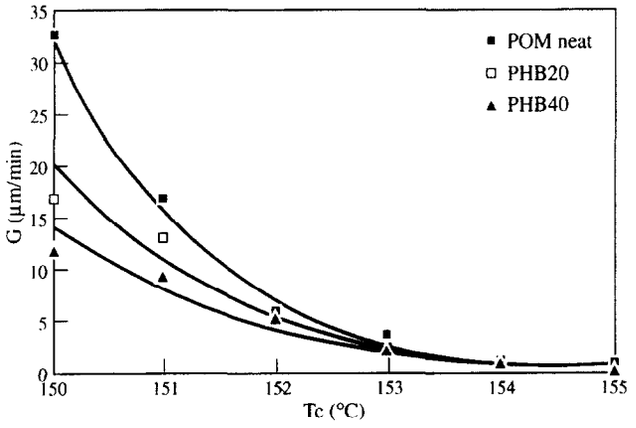

Figure 4 Growth rate, G, of POM spherulites vs crystallization temperature, T_c

Table 1 Melting temperature of the components after isothermal crystallization in the blend

	T_m^{POM} (°C)	T_m^{PHB} (°C)
POM	165	
PHB 20	164	[a]
PHB 40	164	154
PHB 60	163	154
PHB 80	164	154
PHB		170

[a] No visible PHB phase

The trend of the experimental data indicates that the growth rate of POM spherulites, at a prefixed temperature, is reduced in the blends. The diminution of the growth rate, G, is more pronounced at lower temperatures, where the crystallization process is faster.

Being PHB and POM immiscible, the observed depression of the growth rates of POM spherulites in the blends may be explained by the lower thermal conductivity of the molten heterogeneous phase from which they arise[7].

Thermal conductivity is a measure of the velocity at which the heat is removed from a material. Comparing the values of this thermal parameter for PHB ($0.156\,W\,m^{-1}\,°C^{-1}$) and POM ($0.292\,W\,m^{-1}\,°C^{-1}$), it emerges that the former exhibits less tendency to propagate heat.

Thus, the presence of PHB droplets obstructs the loss of crystallization heat from the solid–liquid interface of the POM phase, causing a slow down of the linear growth rate of spherulites.

At least in the range explored, the composition of the blend does not significantly influence the linear growth rate of spherulites of POM. Moreover, by a qualitative evaluation, the presence of liquid PHB does not seem to have any influence on the nucleation density of POM in PHB20 and PHB40 blends. As an example, in *Table 1*, the melting point of the two components, isothermally crystallized first at 150°C and then at 90°C, is reported as a function of the composition. A strong depression of the melting point (about 16°C) of the PHB phase is found in the blends, whereas the melting point of the POM remains practically unchanged. This remarkable decrease of the melting temperature can be attributed to the change of lamellar morphology of the PHB in the blends. In fact, during the crystallization of the POM, the growing spherulites push against the surrounding liquid medium, causing space restrictions affecting the subsequent crystallization of the PHB. This constriction forces the PHB to adopt a greater lamellar thickness, which accounts for the lower melting point found in the blends.

THERMAL ANALYSIS: DIFFERENTIAL SCANNING CALORIMETRY

Non-isothermal crystallization

The samples of PHB/POM blends were subjected to the thermal treatment described in the Experimental part. The resulting d.s.c. curves, as a function of the temperature, at constant scan rate were plotted. As an example, the thermograms relative to the PHB 60 blend are shown in *Figure 5*. Being the melting points of the two components very close, the endothermic curves related to the first and third runs show only one peak, while two exothermic peaks are found in the crystallization run.

The temperatures T_m and T_c corresponding to the maximum of the peaks and the apparent enthalpies ΔH_m and ΔH_c, determined from the area of the peaks for each blend composition, are reported in *Table 2*. The ΔH values are expressed in Joules per gram of blend, while the indices 1 and 2 stand for POM and PHB respectively. From the analysis of the data the following considerations come out:

(i) the apparent melting temperature, T_m, gradually decreases with increasing of the POM content.

Differences between the values of I and III RUN are due to the different thermal history of the samples, being in the case of the I RUN the specimens crystallized by the compression moulding; instead the samples melted during the III RUN were previously d.s.c. crystallized, using a scan rate of 10°C min^{-1};

(ii) the higher the POM percentage, the higher the apparent fusion enthalpy of the blends;

(iii) the temperature T_{c1} corresponding to the maximum of the POM crystallization peak remains almost insensitive to the composition change, while the temperature T_{c2} corresponding to the PHB crystallization is strongly dependent on the composition;

(iv) the apparent enthalpies of crystallization ΔH_{c1} and ΔH_{c2} increase with the increasing of the corresponding component.

Table 2 also reports the total crystallinity content X_c for each composition. The values were calculated by the formula:

$$X_c = \frac{\Delta H_m}{w_1 \Delta H^\circ_{m1} + w_2 \Delta H^\circ_{m2}}$$

where w_1 and w_2 are the weight percentages of POM and PHB respectively, ΔH_m is the apparent fusion enthalpy, ΔH°_{m1} and ΔH°_{m2} are the theoretic fusion enthalpies of the two polymers, 100% crystalline. Literature values of 320[8] J g^{-1} and 146[9] J g^{-1} for ΔH°_m of POM and PHB respectively were used, while the ΔH_m was obtained from the third run.

The resulting value of the crystallinity content X_c decreases with increasing of the POM percentage. Moreover, the values of the fusion and crystallization enthalpies may be obtained by the following additivity rules:

$$\Delta H_m^{calc} = w_1 \Delta H^*_{m1} + w_2 \Delta H^*_{m2} \quad (1)$$

$$\Delta H_c^{calc} = w_1 \Delta H^*_{c1} + w_2 \Delta H^*_{c2} \quad (2)$$

where w_1 and w_2 have the usual meaning, ΔH^*_{m1}, ΔH^*_{c1}, ΔH^*_{m2} and ΔH^*_{c2} are the apparent fusion and crystallization enthalpies of the two neat components, whose experimental values are 147 J g^{-1}, 119 J g^{-1}, 84 J g^{-1} and 66 J g^{-1} respectively (see *Table 2*, III RUN). In *Figure 6*

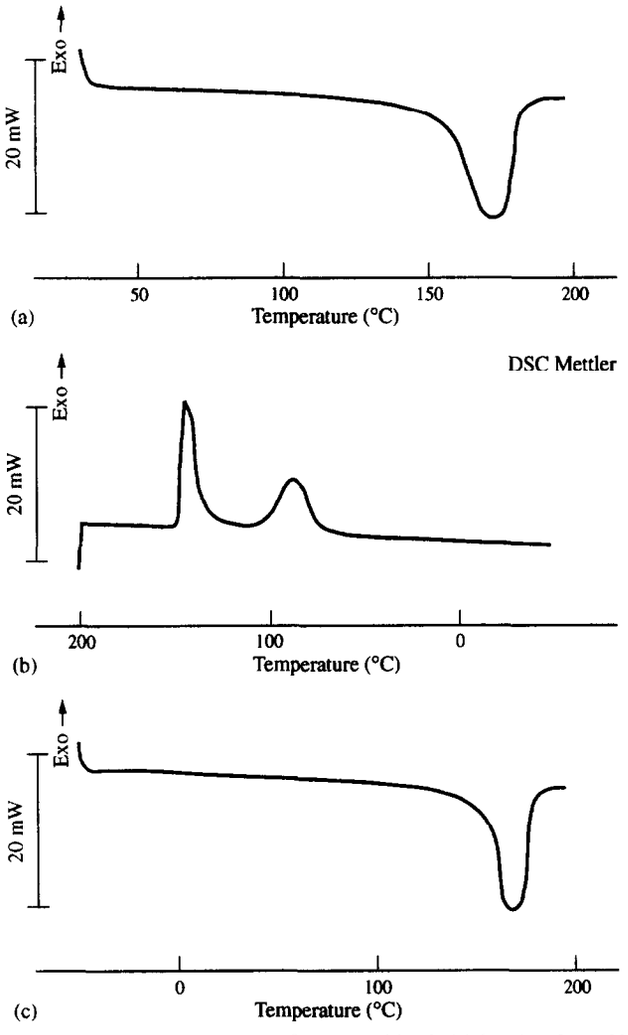

Figure 5 D.s.c. thermograms of PHB 60 blend: (a) heating from 30 to 200°C; (b) cooling from melt to −50°C; (c) re-heating from −50°C to 200°C. The scan rate was 10°C min^{-1}

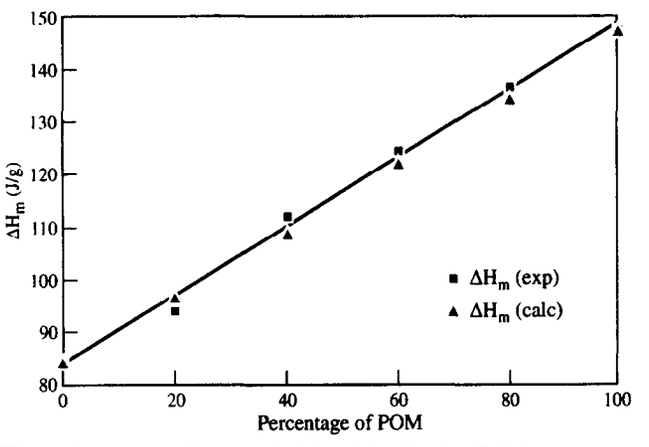

Figure 6 Apparent fusion enthalpies of the blend vs POM percentage: ■, d.s.c. experimental points; (▲) points calculated by assuming a simple additivity

Table 2 D.s.c. parameters for PHB/POM blends

	I RUN		CRYSTALLIZATION RUN				III RUN		
	T_m (°C)	ΔH_m (J g^{-1})	T_{c1} (°C)	T_{c2} (°C)	ΔH_{c1} (J g^{-1})	ΔH_{c2} (J g^{-1})	T_m (°C)	ΔH_m (J g^{-1})	X_c (%)
PHB	176	89	–	95	–	66	175	84	57
PHB 80	173	98	143	92	27	48	173	94	52
PHB 60	172	101	146	89	53	35	169	112	52
PHB 40	172	116	146	83	75	18	169	124	49
PHB 20	171	123	145	44	99	6	168	136	48
POM	170	129	144	–	119	–	166	147	46

is drawn the straight line of the fusion enthalpy of the blends as a function of the composition. The experimental points are reported, together with those coming out from equation (1).

The good agreement between the two sets of values is evidence of the immiscible nature of PHB/POM blends. This finding indicates that changes of the global crystallinity content are only due to the blend composition, while the mixing does not affect the crystallinity of the two components.

Isothermal crystallization

According to Avrami[10], the fraction of crystallinity at time t, $X(t)$, is expressed by the equation:

$$X(t) = 1 - \exp(-Kt^n)$$

where k and n are two constants. In particular, the kinetic constant, k, contains both nucleation and growth parameters, while the Avrami exponent n is nearly an integer whose value depends on the mechanism of nucleation and on the form of crystals.

The Avrami equation can be rewritten in linear form as follows:

$$\log\{-\log[1 - X(t)]\} = b + n\log t$$

where b is equal to $\log(k \cdot \ln 2)$.

It is accustomed to define the overall rate of crystallization as the inverse of the semitransformation time $t_{1/2}$, which is the time needed for development of 50% of the final crystallinity.

The progress of the isothermal crystallization of the blends was followed by d.s.c. measurements at two temperatures: 153°C for POM and 120°C per PHB, according to the procedure described in Experimental.

The crystallinity as a function of the crystallization time was calculated by the formula:

$$X(t) = \int_0^t (\mathrm{d}H/\mathrm{d}t)\mathrm{d}t \Big/ \int_0^\infty (\mathrm{d}H/\mathrm{d}t)\mathrm{d}t$$

where the integral at the numerator is the portion of the area of the exothermic peak developed at time t while the denominator is the total area of the peak.

The quantity $\log[-\log(1 - X(t)]$ was reported against $\log t$ and the experimental data fitted according to the least square method. The Avrami parameters n and k were calculated from the slope and the intercept b of the straight line, b being related to the kinetic constant by the relation:

$$k = 10^b / \ln 2$$

Moreover the value of the semitransformation line was interpolated by placing $X(t) = 0.5$ in the Avrami equation.

To take into account the statistic nature of the crystallization process, for each blend composition six experiments were performed and the values of Avrami parameters averaged.

In *Tables 3a* and *3b* are reported the kinetic parameters such as the Avrami exponent, n, the kinetic constant, k, and the semitransformation time $t_{1/2}$ for the crystallization process performed at 153 and 120°C respectively. Most values of n are non-integer, close to 3, concordant with literature values reported for POM by Cruz-Pinto *et al.*[11]. Such values of the Avrami parameter n indicate an instantaneous three-dimensional nucleation.

Table 3 Crystallization parameters for PHB/POM blends: (a) Avrami exponent, kinetic constant rate and semitransformation time for POM phase crystallized at 153°C; (b) Avrami parameters for PHB crystallized at 120°C

	n	k (s^{-n})	$t_{1/2} \times 10^{-2}$ (s)
(a)			
POM	3.2	2.2×10^{-10}	9.0
PHB 20	3.2	3.6×10^{-10}	9.4
PHB 40	3.1	2.5×10^{-10}	11.1
PHB 60	3.1	1.3×10^{-9}	6.6
PHB 80		No peak	
(b)			
PHB	3.1	5.5×10^{-10}	8.0
PHB 80	3.0	5.5×10^{-10}	9.7
PHB 60	3.1	8.3×10^{-11}	16.1
PHB 40	4.4	2.7×10^{-15}	18.5
PHB 20		No peak	

For the PHB phase in PHB 40 the value of n found, equal to 4.4, is probably due to a decrease of the crystallinity during the final growth of spherulites[12]. As a matter of fact, the Avrami model is only an approximation of the crystallization mechanism of real systems, and thus does not take into account many factors that may determine deviations from theoretical predictions. The observed diminution of crystallinity of spherulites of PHB in their late isothermal growth from PHB 40 should be so slight as to be not appreciable in a dynamic d.s.c. measurement.

Concerning the semitransformation time of PHB, it increases with the increase of the POM content in the blend, indicating a decrease of the nucleation density (number of nuclei per surface unit) and/or of the growth rate of PHB spherulites in the blend. The crystallization of the PHB is so slow at 120°C in the PHB 20 blend that the curve is not detectable by a d.s.c. This behaviour is in agreement with the nucleation study on polyethylene droplets reported by Barham *et al.*[13]. They observed a reluctance of a great part of droplets to crystallize from the melt during cooling. Such droplets had to be cooled to a much lower temperature before they would nucleate and crystallize.

The slow-down of the crystallization rate of the PHB in the blend is expected as a consequence of the diminution of the number of nucleating impurities per number of droplets. The reasons for this diminution may be the finer dispersion grade of the PHB with increasing POM percentage, and/or the migration of a few impurities from PHB to POM. In the same way, the isothermal crystallization peak of POM in PHB 80 blend is not evident because of the extreme dilution of this component.

Concerning the rate of crystallisation of POM in the blends, a more complex pattern is found by changing the composition. Indeed, the global crystallization rate is almost the same for POM, PHB 20 and PHB 40, while PHB 60 exhibits a higher value. This behaviour is in agreement with the microscopic observations that evidenced a phase inversion: an exchange matrix-dispersed component as the percentage of a component exceeds that of the other one. This fact leads to a higher nucleation density in PHB 60 and PHB 80 of the POM phase with respect to PHB 40 and PHB 20. *Figure 7* shows the SEM micrographs of samples crystallized in a d.s.c. calorimetric cell according to the procedure reported in the Experimental part. There can be observed

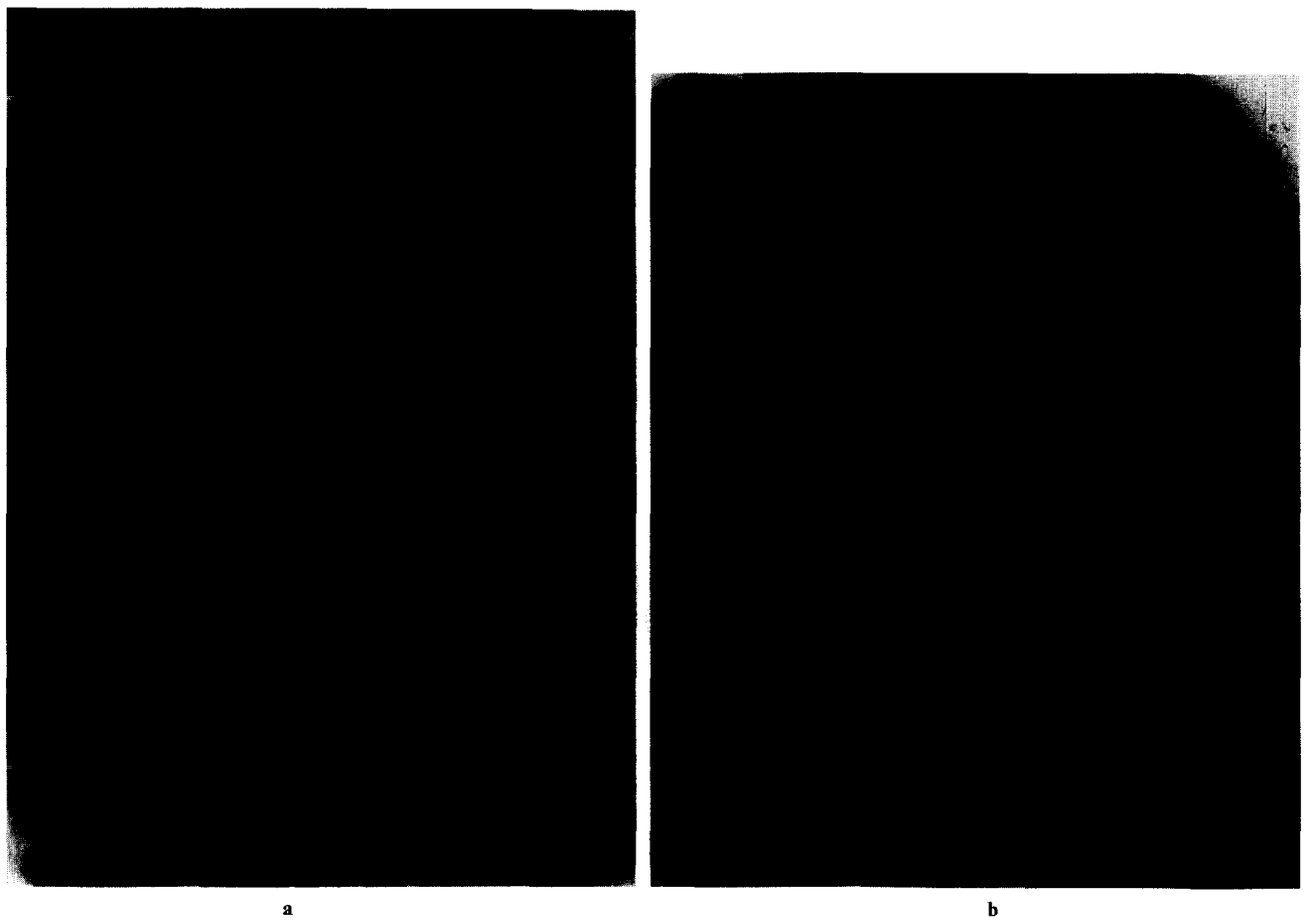

a b

Figure 7 SEM micrographs of d.s.c. isothermally crystallized samples: (a) PHB 40; (b) PHB 60. Magnification 320×

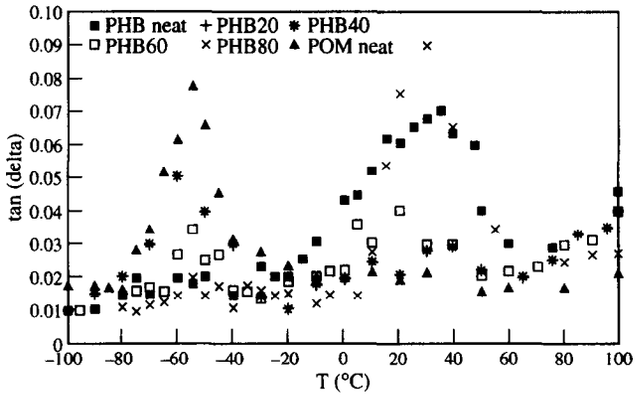

Figure 8 Loss factor of PHB/POM blends as a function of the temperature

a strong reduction of the dimension of POM spherulites in the PHB 60 blend as a consequence of the phase inversion. The average diameter of POM spherulites falls from the order of magnitude of hundreds of microns in the PHB 20 and PHB 40 blends to a few microns in PHB 60 and PHB 80 blends.

It is worth reminding that the global crystallization rate depends both on the nucleation and growth processes. This latter is in turn affected by the rate at which the heat developed by the liquid–solid transition is removed from the growing front.

As observed, the growth rate of POM nuclei markedly decreases in the blends owing to the lower thermal conductivity of the heterogeneous medium in which the crystals arise. Nevertheless the nucleation density may become greater in the presence of PHB, thus contrasting the delay of the overall crystallinity development in the blend. Therefore, for PHB 60 and PHB 80 blends, the influence of the higher nucleation rate prevails upon the lowering of the growth rate; the result is a decrease of the semitransformation time. Instead, in the case of the PHB 20 and PHB 40 blends, the slight diminution of the growth rate of POM spherulites assessed by microscopic observations do not seem to affect the global crystallization rate of POM in bulk.

Table 4 Tensile properties of PHB/POM blends

	Elastic modulus (GPa)	Stress at break (MPa)	Strain at break (%)
PHB	2	28	2.6
PHB 80	1.9	18	1.0
PHB 60	1.9	16	0.9
PHB 40	1.7	13	1.1
PHB 20	1.9	34	4.4
POM	1.9	58	10.7

MECHANICAL PROPERTIES

Mechanical test results and fractographic analysis

In *Figure 8* the dynamic mechanical loss factor vs the temperature of PHB/POM blends is reported. Being very sensitive to the molecular motions, the loss factor exhibits marked peaks relating to the glass transition temperature regions. The presence of two distinct relaxation maxima in the vicinity of −60°C and 30°C

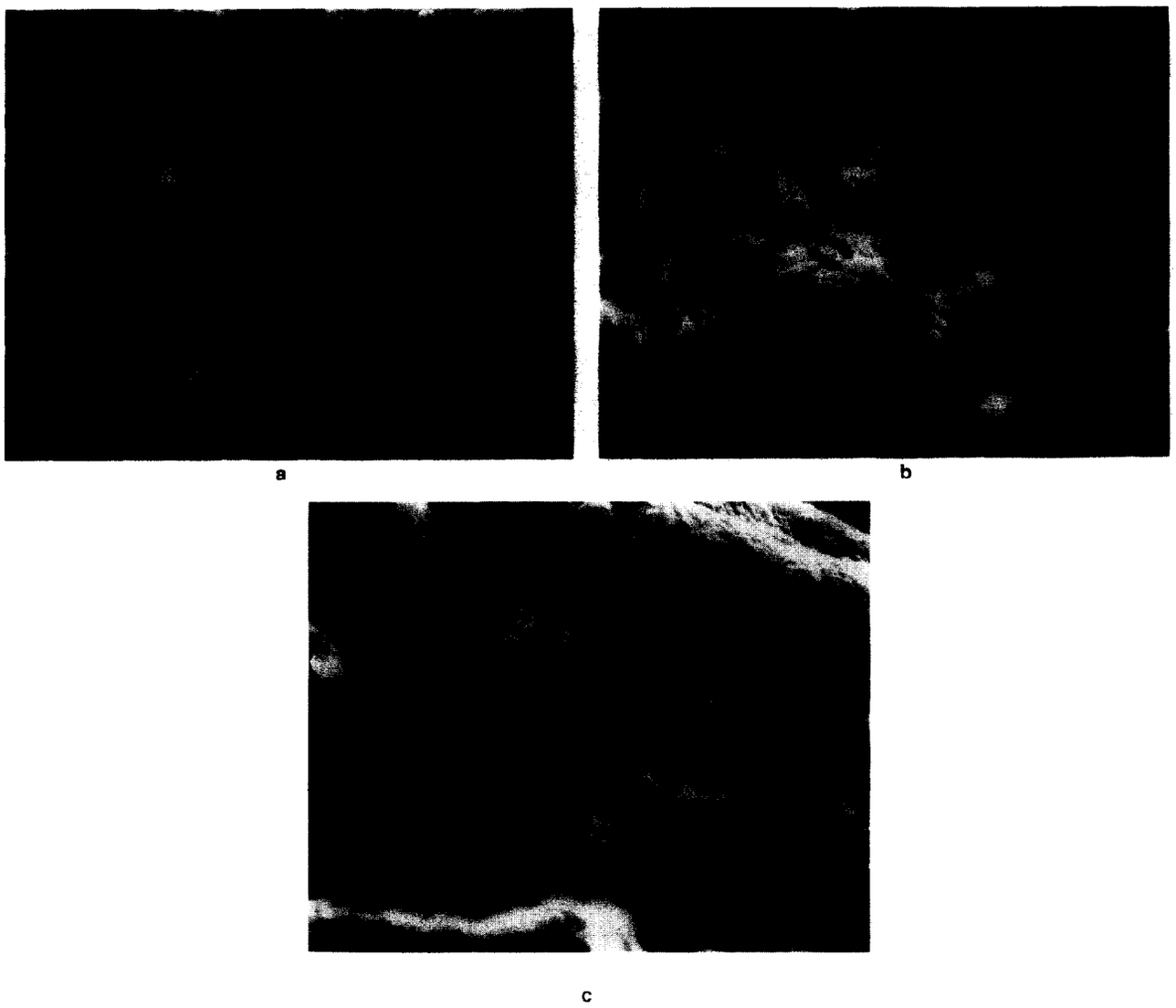

Figure 9 SEM micrographs of fractured surfaces of specimens submitted to tensile test: (a) POM; (b) PHB 20; (c) PHB 40. Magnification 640×

demonstrates the immiscibility of the two polymers in the amorphous phase.

Table 4 reports the elastic modulus, the stress and the strain at break for each blend composition. In *Table 5*, the values of the critical strain energy release rate G_c and the critical stress intensity factor K_c, calculated according to the linear elastic fracture mechanism (LEFM) theory are shown. From the data reported in the tables, the non-compatible nature of the PHB/POM blend is revealed. Indeed, decreased values of the mechanical parameters are found, rather than data fitting a linear trend according to the rule of mixtures, except for Young's modulus, which remains constant with the composition.

The lack of adhesion between the weaker PHB and the more resistant POM makes the resulting blends less tough than neat POM. However, blends of PHB percentage equal to or less than 20% exhibit improved mechanical properties with respect to neat PHB. SEM analysis of samples submitted to tensile test, illustrated in *Figure 9*, has shown a brittle behaviour and a poor adhesion between the two components of the blend. Notwithstanding this, the ellipsoidal shape of the dispersed phase in PHB 20 blends proves a higher grade of toughness. In blends containing a PHB percentage greater than 20%, as PHB 40, bigger particles of PHB having a spherical shape have been revealed, indicating a poor plastic deformation of the material. The same considerations arise from the analysis of the fractured surfaces of samples submitted to impact testing, SEM micrographs of which are shown in *Figure 10*.

Table 5 Fracture parameters of PHB/POM blends

	POM	PHB 20	PHB 40	PHB 60	PHB 80	PHB
K_c (MN m$^{-3/2}$)	3.26	2.98	2.33	1.60	1.71	2.50
G_c (kJ m^{-2})	2.64	2.47	1.46	0.59	0.85	1.29

CONCLUSION

In this work the immiscibility of PHB and POM by investigations on thermal, crystallization and mechanical behaviour of their blends has been demonstrated. Despite their incompatibility, PHB/POM blends are of potential interest because of their wide thermal stability below the unique melting point. Moreover, the mechanical resistance of the blends is not drastically reduced with respect to the separate components.

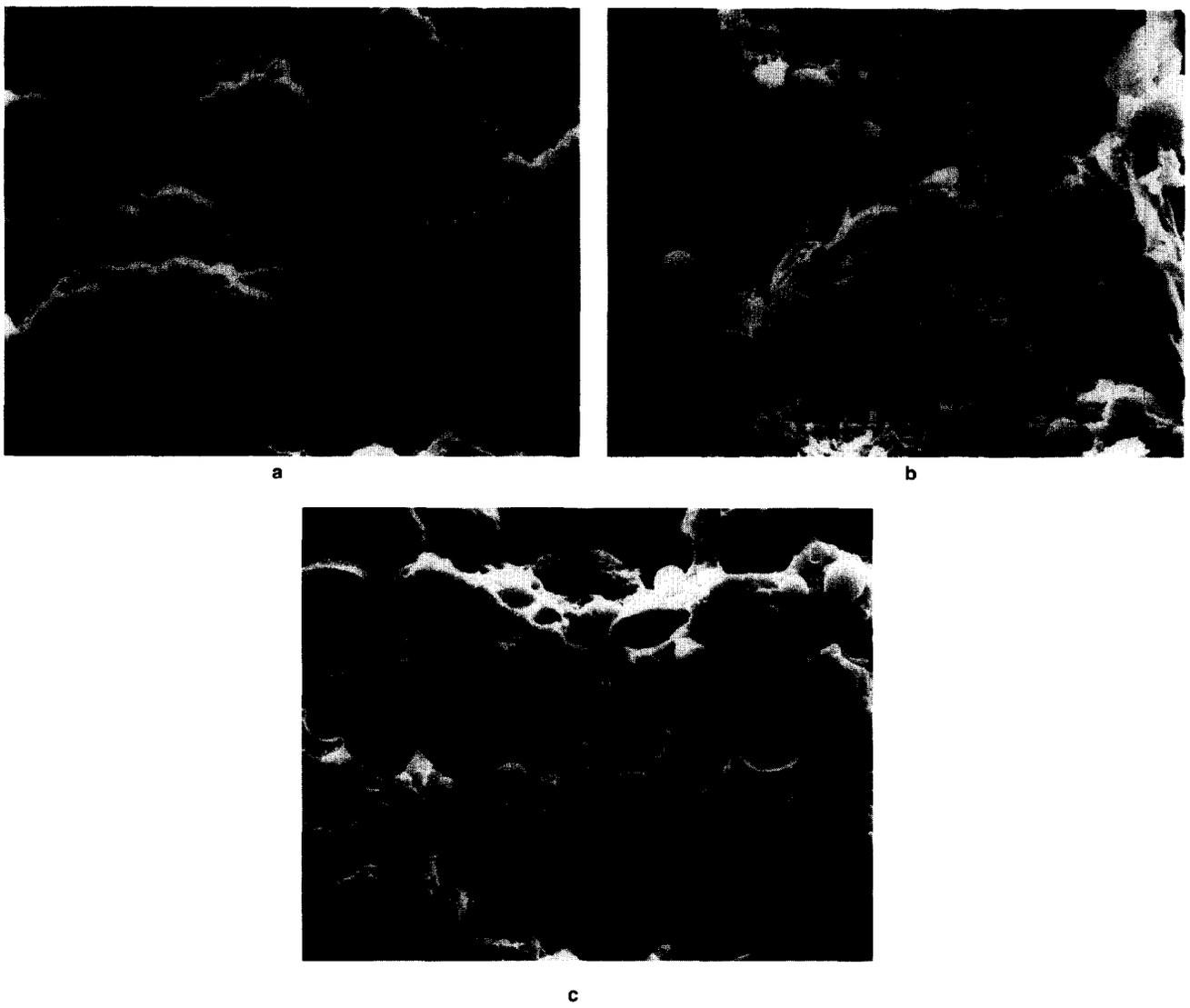

Figure 10 SEM micrographs of fractured surfaces of specimens submitted to impact test: (a) POM; (b) PHB 20; (c) PHB 40. Magnification 640×

These facts encourage continuing studies on the miscibility between PHB and the POM copolymer. Being PEO and PHB miscible, the oxyethylenic linkages in the POM copolymer are expected to act as a compatibilizer for PHB/POM copolymer blends. The choice of such a copolymer should improve the interfacial adhesion and consequently the mechanical performance of the blend. Work is in progress to verify this expectation.

REFERENCES

1. Avella, M. and Martuscelli, E., *Polymer*, 1988, **29**, 1731.
2. Avella, M., Greco, P. and Martuscelli, E., *Polymer*, 1991, **32**, 1647.
3. Avella, M., Martuscelli, E. and Raimo, M., *Polymer*, 1993, **34**, 3234.
4. Barham, P. J., *J. Mater. Sci.*, 1984, **19**, 3826.
5. Wunderlich, B., *Macromolecular Physics*, Vol. 2. Academic Press, 1973.
6. Salaris, F., Turturro, A., Bianchi, V. and Martuscelli, E., *Polymer*, 1978, **19**, 1163.
7. *Introduzione ai Materiali*, Biblioteca della Est-Edizioni Scientifiche e Tecniche-Mondadori, 1976.
8. Brandrup, J. and Immergut, E. H., *Polymer Handbook*, 2nd edn. New York, 1975.
9. Barham, P. J., Keller, A., Otun, E. L. and Holmes, P. A., *J. Mater. Sci.*, 1984, **19**, 2781.
10. Avrami, M., *J. Chem. Phys.*, 1939, **7**, 1193.
11. Cruz-Pinto, J. J. C., Martins, J. A. and Oliveira, M. J., *Coll. Polym. Sci.*, 1994, **272**, 1.
12. Hay, J. N. and Przekop, Z. J., *J. Polym. Sci., Polym. Phys. Edn*, 1979, **17**, 951.
13. Barham, P. J., Jarvis, D. A. and Keller, A., *J. Polym. Sci. Polym. Phys. Edn*, 1982, **20**, 1733.